ISSN (Online) 2395-2717

International Journal of Engineering Research in Electrical and Electronic Engineering (IJEREEE)
Vol 6, Issue 9, September 2020

Structural and Luminescence Studies of Li^+ and Bi^{3+} ion Doped $Y_2O_3:Eu^{3+}$ Tunable Red-Emitting Nanophosphors for White-LEDs

[1] Sanjeeb Limbu, [2]Laishram Robindro Singh

[1][2] Department of Nanotechnology, North-Eastern Hill University, Shillong-793022, India

Abstract— **This work reports structural and luminescence properties of tunable $Y_2O_3:Eu^{3+}$ red-emitting nanophosphors sensitized with Li^+ and Bi^{3+} by wet chemical method. The structural property followed by X-ray diffraction analysis shows the nanophosphors have a body-centered cubic (I) phase with space group Ia-3 and point group symmetry m-3. No additional impurity peaks were observed within the range of the XRD pattern due to the Li^+ and Bi^{3+} ion. The unit cell structure of cubic Yttrium oxide (Y_2O_3) was modeled by using Rietveld refinement XRD data. The photoluminescence study shows the most intense red emission band at 612 nm due to the $^5D_0 \rightarrow {}^7F_2$ transition of Eu^{3+} ion in the C_{3i} and C_2 symmetry site of Y_2O_3 respectively. The emission band of Li^+ codoped $Y_2O_3:Eu^{3+}$ nanophosphor shows 2.97 times enhancement than the $Y_2O_3:Eu^{3+}$ one because of the flux effect created by Li^+ ion. The Bi^{3+} codoped $Y_2O_3:Eu^{3+}$ nanophosphor shows the most intense band as compared to the other bands and is due to the energy transfer from Bi^{3+} to Eu^{3+} ion. It shows 6.56 times higher enhancement than the emission band corresponds to $Y_2O_3:Eu^{3+}$ nanophosphor. The average lifetime was found to vary based on the different sensitizers used. The calculated Commission Internationale de l'Eclairage (CIE) 1931 chromaticity coordinates and correlated color temperature (CCT) values were tuned in the red region of the color space. All the results indicate that the prepared nanophosphor can be used as a potential red component to construct the white light for white light-emitting diodes fabrication.**

Keywords - White light-emitting diode, Photoluminescence, Chromaticity, Nanophosphors

1. INTRODUCTION

Since the last few decades, Rare earth (RE) ion doped luminescence materials have been attracted broad research interest, due to their potential applications in various fields. Eu^{3+} doped Y_2O_3 materials have been widely used as a red phosphor component in the white-light-emitting diode, plasma display panels (PDP), field emission display (FED), cathode ray tube (CRT) [1-3]. The Eu^{3+} ion can exhibit both the divalent and trivalent valance state among the all RE element. Therefore, Eu^{3+} doped phosphors are use to produce tricolors blue, green, and red depends on different host materials [4]. The Eu^{3+} ion reveals the prominent red emission band due to the $^5D_0 \rightarrow {}^7F_2$ transition [5]. Therefore, the Eu^{3+} ion has been widely used as a dopant in different nanophosphors because it is having some special characters.

Luminescence property of Eu^{3+} doped of the red-emitting phosphors has been studied for the last several decades. To improve the crystallinity and enhanced the emission band intensity of the rare earth doped phosphors, different metal ions were added into the phosphors. The Li^+ ion serves as flux materials to improve luminescence efficiency and enhanced the emission band intensity [6, 7]. It created the oxygen vacancy in the phosphors material. In the case of Bi^{3+} ion-doped $Y_2O_3:Eu^{3+}$ nanophosphor is generally using as a white emitting nanophosphor for LEDs fabrication. This phosphor shows three standard emissions band for red (R), green (G) and blue (B) colors. Finally, these RGB colors are combined to construct white light for further LED applications.

ISSN (Online) 2395-2717

International Journal of Engineering Research in Electrical and Electronic Engineering (IJEREEE)
Vol 6, Issue 9, September 2020

In this work, we have studied the structural and luminescence properties of $Y_2O_3:Eu^{3+}$ red-emitting nanophosphrs sensitized with Li^+ and Bi^{3+} ions. The structural study followed by XRD analysis shows the nanophosphors have a pure body-centered cubic (I) phase with point group symmetry m-3. No additional impurity peaks were observed within the whole range of the XRD pattern due to the addition of Li^+ and Bi^{3+} ions. By observing the photoluminescence intensity Bi^{3+} codoped $Y_2O_3:Eu^{3+}$ nanophospor shows the highly intense emission band as compared to the other band. The CIE 1931 chromaticity coordinates tuned the prepared nanophosphor are located in the red region of the color space.
These obtained results indicate that the prepared nanophosphors can be used as a red component for white-LEDs fabrication.

METHODOLOGY

The Y_2O_3:4at.%Eu^{3+} nanophosphors sensitized with 4at.%Li^+ and 4at.%Bu^{3+} were prepared by the conventional wet chemical methods [8]. The Yttrium (III) acetate hydrate $(CH_3.CO_2)_3Y.xH_2O$ (Alfa Aesar 99.99%), Europium (III) oxide (Eu_2O_3) (Sigma Aldrich 99.99%), Lithium Acetate ($C_2H_3LiO_2$) (Sigma-Aldrich, 99.95%, Purity) and Bismuth (III) nitrate pentahydrate $(BiNO_3)_3.5H_2O$ (AR, 98%) were used to prepare the nanophosphors. At first, 0.5 g Yttrium (III) acetate hydrate $(CH_3.CO_2)_3Y.xH_2O$ (Alfa Aesar 99.99%) and the calculated amount of Eu_2O_3 (Sigma Aldrich 99.99%) were mixed with 10 ml of dilute hydrochloric acid. The mixtures were stirred vigorously to get a clear solution. The solution was evaporated several times in double distilled water to remove excess acids from the solution. The solution was poured into a 250 ml round bottom flask having a condenser. Polyethylene glycol of 25 ml was added and warms the solution until it got clear. Then, 1M strength sodium hydroxide (AR) was added into the observed clear solution and heated continuously the mixture up to 140 °C. The solution observed as foggy white precipitate and continued the reaction for three hours. To remove the additional ligands, the forming white precipitate was washed several times using double distilled water and methanol under the centrifugation process. Finally, the residue was collected and considered as Y_2O_3:4at.%Eu^{3+} nanoparticles. To incorporate 4at.% Li^+ or 4at.% Bi^{3+} ions in Y_2O_3:4 at.% Eu^{3+}, Lithium Acetate or Yttrium (III) acetate hydrate was initially dissolved in double distilled water to get Li^+/Bi^{3+} ions and is simply added into the mixture of Y^{3+} and Eu^{3+} and follows the same procedure were followed as to prepare Y_2O_3:4at.% Eu^{3+} nanoparticles. The prepared sample was annealed at 900 ℃ for 3h. These synthesized nanomaterials were kept continuously in the furnace for cool down to room temperature and ground for further characterization to observe the structural and luminescence properties.

X-ray diffraction (XRD) data were obtained by Explorer, GNR Instrument and Analysis, Italy using Cu Kα radiation source and a monochromatic wavelength (λ = 1.5406 Å) operating at 40 kV tube voltage and 35 mA tube current with 2θ angle ranging from 10 to 80°. The Rietveld refinement quantitative structural analysis was conducted using the FullProf Suite software package. The Photoluminescence (PL) measurements were observed on a Hitachi F-7000 Fluorescence Spectrophotometer at room temperature with slit width kept open for 3 nm, having a 150 W Xe arc lamp as an excitation light source. The Commission Internationale de l'Éclairage (CIE) 1931 color calculator was used to evaluating the chromaticity color coordinates (x, y) from the PL emission spectra.

RESULTS AND DISCUSSION

Figure 1(a) represents the X-ray diffraction (XRD) patterns of $Y_2O_3:Eu^{3+}$, Li^+/Bi^{3+} nanophosphors. All the diffraction peaks were matched with the International Centre for Diffraction Data (ICDD) Card No. 41-1105, no additional peaks were observed within the range of the XRD pattern. The XRD pattern confirms that the crystallographic structure of doped and codoped Y_2O_3 nanoparticles is a cubic structure with Ia-3 (Number 206, Z=16) space group. There was no impure peak and phase change could be detected within the whole range of Eu^{3+} and Li^+/Bi^{3+} ions concentration. The average crystallite size (D) was calculated by using the Debye Scherrer relation, $D=k\lambda/\beta\cos\theta$, here k = 0.9 is the dimensionless shape factor (Scherrer constant), λ =1.5406 Å is the wavelength of X-ray radiation used, β is the full width at half maxima (FWHM), θ is the Bragg diffraction angle. To calculate the crystallite size, the most intense was selected corresponding to the plane (222).

ISSN (Online) 2395-2717

International Journal of Engineering Research in Electrical and Electronic Engineering (IJEREEE)
Vol 6, Issue 9, September 2020

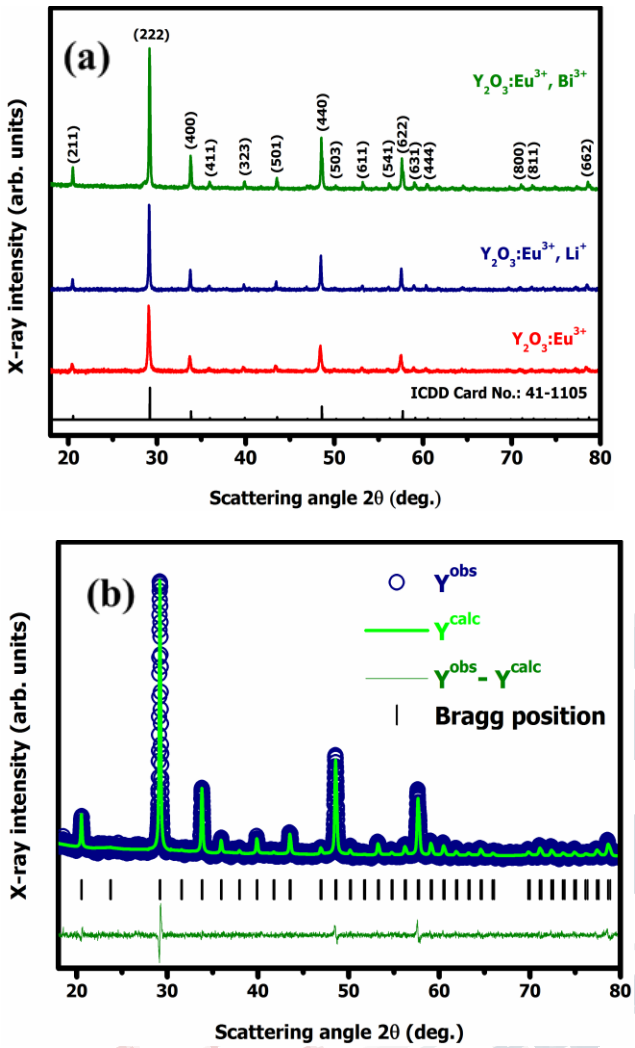

FIGURE 1. XRD pattern for (a) $Y_2O_3:Eu^{3+}$, $Y_2O_3:Eu^{3+}$, Li^+ and $Y_2O_3:Eu^{3+}$, Bi^{3+} nanophosphor (b) Rietveld refined XRD pattern of $Y_2O_3:Eu^{3+}$ nanophosphors.

Based on this relation, the calculated average crystallite sizes of $Y_2O_3:Eu^{3+}$, $Y_2O_3:Eu^{3+}$, Li^+ and $Y_2O_3:Eu^{3+}$, Bi^{3+} nanophosphors are accordingly 36.76 nm, 54.54 nm and 58.07 nm, respectively. All the crystallographic and diffraction data of $Y_2O_3:Eu^{3+}$, Li^+ nanophosphors are summarized in Table 1. The crystallite size of nanophosphor was found increased with the addition of Li^+ and Bi^{3+} into the $Y_2O_3:Eu^{3+}$ nanophosphor, which indicates the variations of lattice parameters in the lattice crystal. The quantitative XRD analysis of the $Y_2O_3:Eu^{3+}$ nanophosphors were performed by the Rietveld refinement method [9]. All the structural parameters were evaluated through the FullProf Suite crystallographic program using powder XRD data. The obtained structural refined parameters are tabulated in Table 2. The Pseudo-Voigt function was utilized to fit various parameters to the data point. The patterns were typically fitted with parameters such as backgrounds, cell parameters; scale factor, zero shifting, shape and width of the peaks, atomic coordinates, isothermal temperature factors, and asymmetric factors. The refinement result exhibited that nanophosphors have a body-centered cubic (I) phase with point group symmetry m-3. The fitting parameters R_{wp}, R_{ex}, GoF, R_p, R_{Bragg}, R_F, and χ^2 were also shown a good agreement with the observed and calculated XRD patterns. The observed, calculated, and difference between observed and calculated XRD patterns for nanophosphors are shown in fig. 1(b). The quality of refinement data was examined by the lower values of the goodness of fit (GoF) which is given by the ratio of expected and weighted profile of R factors i.e., GoF = $R_{wp}/R_{exp.}$ For the perfect refinement, GoF must approach to unity. In this case, GoF values were found to be 1.12, 1.20 and 1.29, respectively which indicates our fitting is best. By observing unit cell volume, it increases with different codopant, which indicates variations of the lattice parameters within the lattice crystal.

TABLE 1. Crystallographic and diffraction data of $Y_2O_3:Eu^{3+}$ nanophosphors.

Crystallographic Data		Diffraction Data				
Crystallographic Parameters	Structure and Values	Major Peaks 2Th. [°]	FWHM 2Th. [°]	d-spacing [Å]	Rel. Int.	hkl
Crystal System	Cubic	20.46	0.3487	4.3479	123.0	211
Cell Parameter	a=10.6502 Å	29.00	0.3599	3.0744	1000.0	222
Symmetry Sites	C_2 and C_{3i}	33.65	0.3508	5.3251	219.9	400
Space group	Ia-3	43.39	0.3685	2.0886	73.9	501
Space group number	206	48.30	0.4025	1.8827	294.0	440
Point Group	m-3	57.40	0.3864	1.6055	207.0	622

ISSN (Online) 2395-2717

International Journal of Engineering Research in Electrical and Electronic Engineering (IJEREEE)
Vol 6, Issue 9, September 2020

TABLE 2. Reitveld refinement parameters of $Y_2O_3:Eu^{3+}$ nanophosphors.

Compound	Rietveld Refinement Parameters							
	R_{wp}	R_{exp}	GoF	R_p	R_{Bragg}	R_F	χ^2	Cell Volume a^3(Å)
$Y_2O_3:Eu^{3+}$	26.3	24.0	1.1	53.0	7.33	4.63	1.12	1190.55
$Y_2O_3:Eu^{3+}$, Li^+	24.7	21.8	1.1	44.2	6.91	4.04	1.20	1192.81
$Y_2O_3:Eu^{3+}$, Bi^{3+}	23.0	19.7	1.1	32.4	6.53	6.31	1.29	1193.04

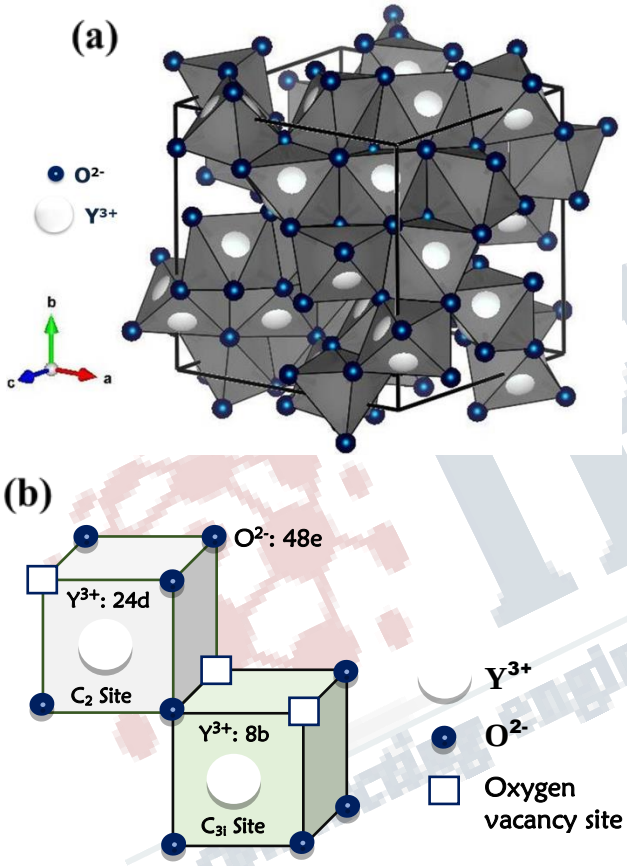

FIGURE 2. (a) schematic representation of the Y_2O_3 unit cell and (b) cationic symmetry site for the $Y_2O_3:Eu^{3+}$ nanophosphor.

Figure 2(a) illustrates the crystallographic structure of cubic Yttrium (III) oxide (Y_2O_3) with an Ia-3 space group

similar to bixbyite containing 16 formula units in the unit cell. Each unit cell has 32 cationic sites with coordination number 6 which are the summation of two partially distributed cation $Y^{3+}(1)$ located at 24d site (Wyckoff position) with C_2 (noncentrosymmetric) symmetry and $Y^{3+}(2)$ located at 8b (Wyckoff position) site with C_{3i} (centrosymmetric) inversion symmetry of the crystallographic lattice. Oxygen ions were occupied at the 48e site (Wyckoff position) of the Y_2O_3 host lattice, which is presented in fig. 2(b). In the Y_2O_3 crystal structure, both the cations $Y^{3+}(C_2)$ and $Y^{3+}(C_{3i})$ have made six-fold octahedral coordination with oxygen thus forming the $[YO_6]$ octahedron structure having 8 faces, 12 edges and 6 vertices. The noncentrosymmetric sites are less symmetric than the centrosymmetric ones.

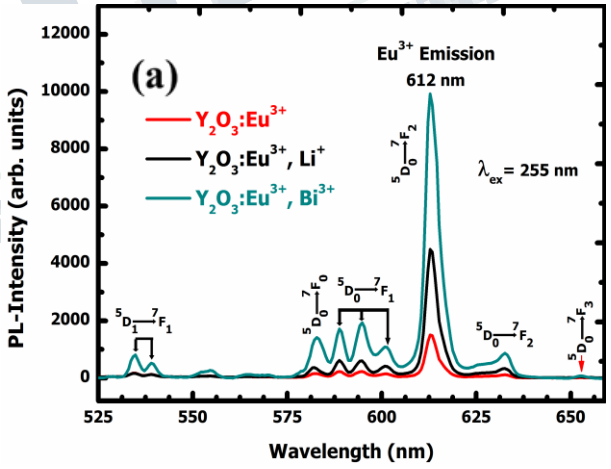

ISSN (Online) 2395-2717

International Journal of Engineering Research in Electrical and Electronic Engineering (IJEREEE)
Vol 6, Issue 9, September 2020

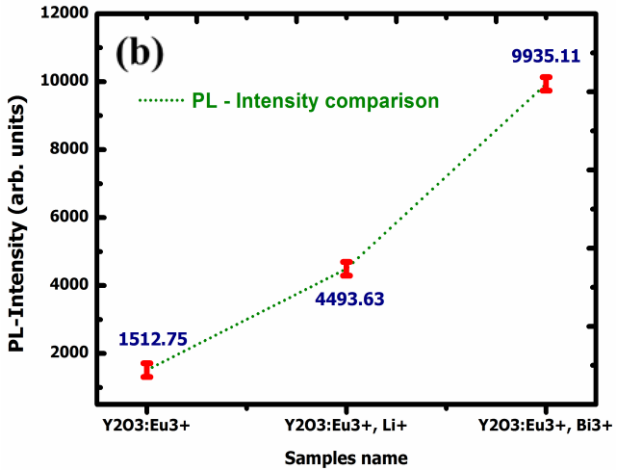

FIGURE 3. (a) PL Emission spectra of Y_2O_3:Eu^{3+}, Y_2O_3:Eu^{3+}, Li^+ and Y_2O_3:Eu^{3+}, Bi^{3+} nanophosphors under excitation 255 nm and (b) PL emission intensity variation curve under $^7F_0 \rightarrow {}^5D_2$ transition of the prepared nanophosphors.

Figure 3(a) depicts the PL emission spectra of Y_2O_3:Eu^{3+}, Y_2O_3:Eu^{3+}, Li^+ and Y_2O_3:Eu^{3+}, Bi^{3+} nanophosphors under excitation 255 nm. The emission bands exhibited at ~534 and 538 nm were ascribed to the hypersensitive electric dipole $^5D_1 \rightarrow {}^7F_1$ transition of Eu^{3+} ion. This indicates the thermalisation takes place within $^5D_1$ multiplet due to the stark splitting. The emission band observed at 582 nm was attributed to a $^5D_0 \rightarrow {}^7F_0$ electric dipole transition, which specifies that Eu^{3+} ion does not occupy in a centrosymmetric site of the host lattice. It occupies only C_3 and C_s noncentrosymmetric sites of the following symmetries: C_s, C_1, C_2, C_3, C_4, C_6, C_{2v}, C_{3v}, C_{4v}, and C_{6v} according to electric dipole selection rule [10]. The emission bands exhibited at ~588, 594, and 600 nm is ascribed to the magnetic dipole transition of $^5D_0 \rightarrow {}^7F_1$ at 8b crystallographic cation site and C_{3i} (centrosymmetric) symmetry of Y_2O_3 (25%) host lattice. The most prominent red emission band at 612 nm and a small band at 632 nm were attributed to the $^5D_0 \rightarrow {}^7F_2$ hypersensitive forced electric dipole transition of Eu^{3+} ion at 24d crystallographic cation site and C_2 (noncentrosymmetric) symmetry of Y_2O_3 (75%) host lattice. This indicates that Eu^{3+} ions were occupying in two separate positions in the crystallographic lattice. The other weak emission band exhibit at 652 nm corresponding to the electric dipole or quadrupole and the magnetic dipole is a forbidden transition of $^5D_0 \rightarrow {}^7F_3$, according to Judd-Ofelt theory. This is because of J- mixing, where the wave function of $^7F_3$ state mixes with another $^7F_{j=2,4,6}$ state. These narrow emission bands were revealed due to the shielding effect of 4f electrons by 5s and 5p in the outer shell in the Eu^{3+} ion. By observing the red emission intensity bands of Y_2O_3:Eu^{3+}, Li^+ nanophosphor under $^5D_0 \rightarrow {}^7F_2$ transition, it shows 2.97 times enhancement than the Y_2O_3:Eu^{3+} one. The enhancement of emission band intensity is also indicated the presence of lattice imperfection in the crystal system. An increment of lattice imperfection indicates the increases in oxygen vacancies due to the flux effect created by co-dopant Li^+ ion. The red emission intensity band of Y_2O_3:Eu^{3+}, Bi^{3+} nanophosphor shows 6.56 times enhancement than intensity band corresponds to Y_2O_3:Eu^{3+} nanophosphor. This is due to the energy transfer from Bi^{3+} to Eu^{3+} ions which is shown in fig. 3(b).

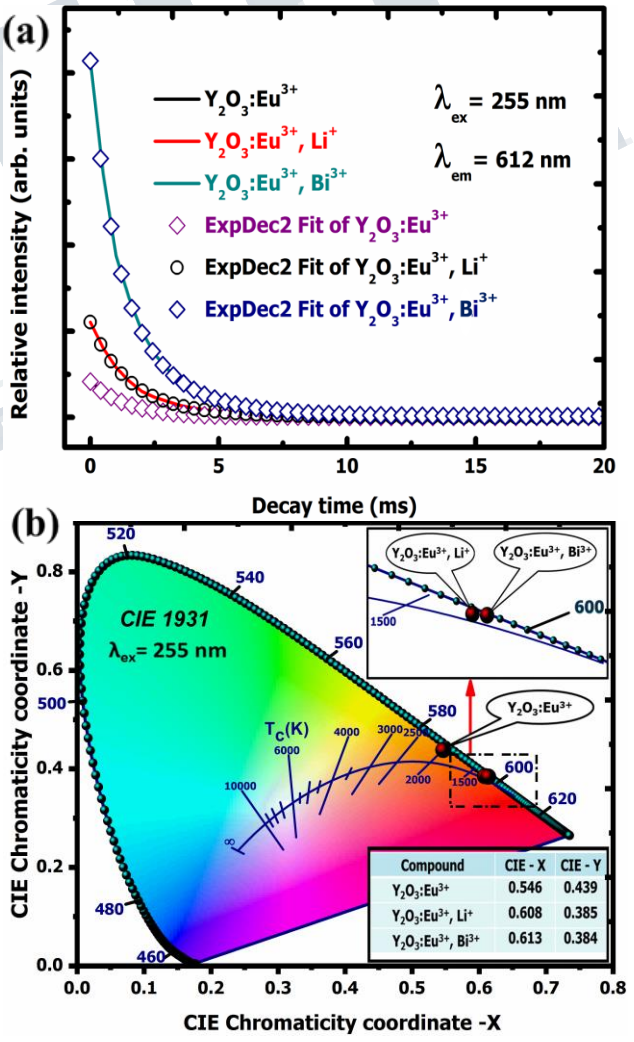

ISSN (Online) 2395-2717

International Journal of Engineering Research in Electrical and Electronic Engineering (IJEREEE)
Vol 6, Issue 9, September 2020

FIGURE 4. (a) PL Life time decay curves of $Y_2O_3:Eu^{3+}$, $Y_2O_3:Eu^{3+}$, Li^+ and $Y_2O_3:Eu^{3+}$, Bi^{3+} nanophosphors (b) The CIE 1931 Chromaticity diagram of $Y_2O_3:Eu^{3+}$, $Y_2O_3:Eu^{3+}$, Li^+ and $Y_2O_3:Eu^{3+}$, Bi^{3+} nanophosphors excited by 255 nm.

Figure 4(a) represents the photoluminescence decay behavior of $^5D_0 \rightarrow {}^7F_2$ (λ_{em}=612 nm) transition of Eu^{3+} for $Y_2O_3:Eu^{3+}$, $Y_2O_3:Eu^{3+}$, Li^+ and $Y_2O_3:Eu^{3+}$, Bi^{3+} nanophosphors excited at 255 nm. All these monitored curves were excellently fitted by a second-order exponential function, $I(t) = I_o + A_1 \exp(-t/\tau_1) + A_2 \exp(-t/\tau_2)$, where I_o and I(t) denoted the luminescence emission intensity at time 0(s), and t(s), respectively, t is time constant, τ_1 and τ_1 represents the fast and slow decay times for exponential components, A_1 and A_2 are assigned fitting parameters constants. The fast and slow decay is assigned non-radiative and radiative transition of Eu^{3+} ion of the nanophosphor. The average lifetimes for the studied nanoposphors were evaluated by using the relation, $\tau_{avg} = (A_1\tau^2_1 + A_2\tau^2_2)/(A_1\tau_1 + A_2\tau_2)$ [11]. Thus, the average lifetime τ_{avg} values of $Y_2O_3:Eu^{3+}$, $Y_2O_3:Eu^{3+}$, Li^+ and $Y_2O_3:Eu^{3+}$, Bi^{3+} nanophosphors found to be 1.44, 1.72 and 2.03 ms, respectively. It is observed that the average lifetimes of the nanophosphors are varying with the co-doping concentration of Li^+ and Bi^{3+} ions. This is because of the flux effect caused by Li^+ ion, which improved the high crystallinity of the sample and the energy transfer from Bi^{3+} to Eu^{3+} ions.

Figure 4(b) represents the Commission Internationale de l'Eclairage (CIE) 1931 chromaticity diagram of $Y_2O_3:Eu^{3+}$, $Y_2O_3:Eu^{3+}$, Li^+ and $Y_2O_3:Eu^{3+}$, Bi^{3+} nanophosphors excited by 255 nm. The calculated CIE chromaticity coordinates and CCTs were calculated based on the photoluminescence color emission spectra. The kelvin (K) based CCT values were obtained by using McCamy's third-order polynomial equation, $CCT = 449n^3+3525n^2+6823.3n+ 5520.33$, where $n = (x-x_e)/(y_e-y)$ is an inverse slope line, (x, y) presents the color coordinates of the prepared nanophosphors and the chromaticity epicentre is at x_e= 0.332 and y_e = 0.185 [12]. All the calculated color coordinates were located within the red region of the color space. The CCT values of $Y_2O_3:Eu^{3+}$, $Y_2O_3:Eu^{3+}$, Li^+ and $Y_2O_3:Eu^{3+}$, Bi^{3+} nanophosphors were found to be 2385.64 K, 167.18 K and 1649.78 K, respectively, which indicates the formation of the red color. The colorimetric performance shows that this nanophosphor can be used as a prominent red component to construct white light for WLED fabrication.

CONCLUSION

In this work, we have presented the structural and luminescence study of tunable $Y_2O_3:Eu^{3+}$ red-emitting nanophosphors sensitized with Li^+ and Bi^{3+} ions. X-ray diffraction pattern shows the formation of pure body-centered cubic phase of Y_2O_3 with Ia-3 (Number 206, Z=16) space group without impurity peaks and which indicates there is no effect sensitizers on it. The crystallite size of $Y_2O_3:Eu^{3+}$, $Y_2O_3:Eu^{3+}$, Li^+ and $Y_2O_3:Eu^{3+}$, Bi^{3+} nanophosphors are found to be 36.76 nm, 54.54 nm and 58.07 nm, respectively. The Rietveld refinement analysis shows the nanophosphors have good crystallinity with point group symmetry m-3. The PL emission intensity shows the most intense emission band at 612 nm ascribed to the $^5D_0 \rightarrow {}^7F_2$ transition of Eu^{3+} ion. The PL emission intensity is found greatly depends on the sensitizers used. The emission band excited of $Y_2O_3:Eu^{3+}$, Bi^{3+} nanophosphors shows the highly enhanced luminescence intensity tan the others. The CIE chromaticity color coordinates, CCTs of all prepared nanophosphors were found located in the red region of the color space. This indicates that the nanophosphors can be used as a red-emitting component for WLEDs applications.

REFERENCES

[1] M. I. Martinez-Rubio, T. G. Ireland, G. H. Fern, J. Silver and M. J. Snowden, *Langmuir*, 2001, 17, 7145-7149.
[2] W.-C. Chien, Y.-Y. Yu and C.-C. Yang, *Mater. Des.*, 2010, 31, 1737-1741.
[3] J. H. Zhang, Z. D. Hao, J. Li, X. Zhang, Y. Luo and G. Pan, *Light Sci. Appl.*, 2015, 4, 239-244.
[4] C. Liang, X. Huang and W. Huang, *J. Mater. Sci.: Mater. Electron.*, 2018, 29, 11271-11279.
[5] Q. Zhang, X. Wang, X. Ding and Y. Wang, *Inorg. Chem.*, 2017, 56, 6990-6998.
[6] Z. Sun, Y. Zhou and M. Li, *J. Mater. Res.*, 2008, 23, 732-736.
[7] M. Peng, X. Yin, P. A. Tanner, C. Liang, P. Li, Q. Zhang and J. Qui, *J. Am. Ceram. Soc.*, 2013, 96, 2870-2876.
[8] L. R. Singh, R. S. Ningthoujam, V. Sudarsan, I. Srivastava, S. D. Singh, G. K. Dey and S. K. Kulshrestha, Nanotechnology, 2008, 19, 055201-8.
[9] M. Ferrari and L. Lutterotti, *J. Appl. Phys.* 1994, 76, 7246-7255.

[10] X. Y. Chen, G. K. Liu, *Solid*. *State*. *Chem*. 2005, 178, 419-428.
[11] C. K. Lin, M. L. Pang, M. Yu and J. Lin, *J. Lumin*. 2005, 114, 299-306.
[12] C. S. McCamy CS, Color Res. Appl. 1992, 17, 142-144..